Service

Author Profile

"The best advice I have ever been given is to follow my heart.
I like refereeing because it is an excellent way to stay up-to-date in the research field. …"
This and more about Gerard Meijer can be found on page 10930.

News

G. S. Fischer

E. Winterfeldt

G. Mloston

C. Ottmann

A. Walther

X. Duan

J. Seibel

E. W. Meijer

P. Schwille

M. Mann

Books

Highlights

Asymmetric Catalysis

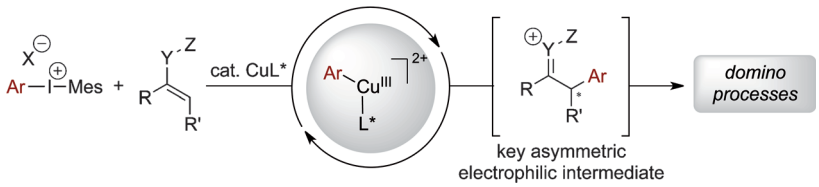

"Chiral aryl cation" equivalents: The combination of diaryliodonium salts and catalytic amounts of chiral copper complexes provides facile access to "chiral aryl cation" synthons. These reagents offer new possibilities for asymmetric arylation reactions that initiate further domino processes.

Step by step: According to the molecular approach to the production of graphene, precursor molecules are cross-linked to form two-dimensional intermediates, and pyrolysis transforms the intermediates into graphene. This type of highly efficient synthesis of high-quality graphene is crucial to the development of innovative applications.

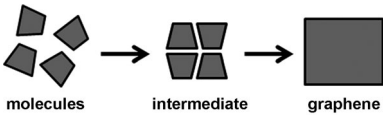

Minireviews

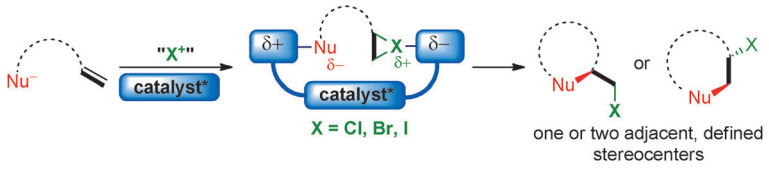

The return of the salt makers: Catalytic enantioselective versions of halofunctionalizations have recently appeared and although important breakthroughs, they represent just the very beginnings of a nascent field. Herein is a critical analysis of the challenges that accompany the development of general and highly enantioselective halofunctionalizations. Various modes of catalysis and the different strategies implemented for asymmetric induction are identified.

Reviews

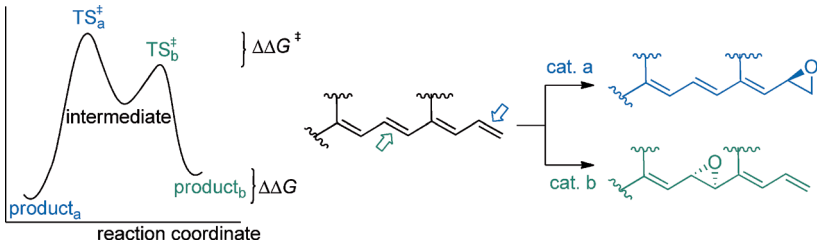

A tale of two catalysts: Catalyst-controlled selectivity is well established for enantioselective catalysis but less formulated for catalytic regio-, chemo,- or product-selective reactions. This Review describes selective transformations of the same starting materials into two or more different products simply by the choice of catalyst even when the reaction conditions are nearly identical.

For the USA and Canada:
ANGEWANDTE CHEMIE International Edition (ISSN 1433-7851) is published weekly by Wiley-VCH, PO Box 191161, 69451 Weinheim, Germany. Air freight and mailing in the USA by Publications Expediting Inc., 200 Meacham Ave., Elmont, NY 11003. Periodicals postage paid at Jamaica, NY 11431. US POSTMASTER: send address changes to *Angewandte Chemie*, Journal Customer Services, John Wiley & Sons Inc., 350 Main St., Malden, MA 02148-5020. Annual subscription price for institutions: US$ 11.738/10.206 (valid for print and electronic / print or electronic delivery); for individuals who are personal members of a national chemical society prices are available on request. Postage and handling charges included. All prices are subject to local VAT/sales tax.

Communications

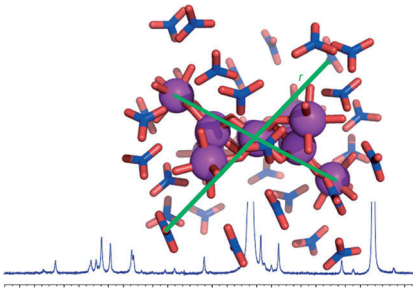

A solved structure: The hydrated Ga_{13} cluster, $[Ga_{13}(\mu_3\text{-}OH)_6(\mu\text{-}OH)_{18}(H_2O)_{24}](NO_3)_{15}]$, persists as a discrete nanoscale structure in an aqueous polar solvent at millimolar concentration. SAXS data confirm the presence of Ga_{13} in dimethyl sulfoxide (DMSO). In aqueous $[D_6]$DMSO ^{1}H NMR signals for the hydroxo and aquo ligands of Ga_{13} were detected, thus showing a cluster with a hydrodynamic radius of (11.2 ± 0.8) Å (see picture).

Structure Elucidation

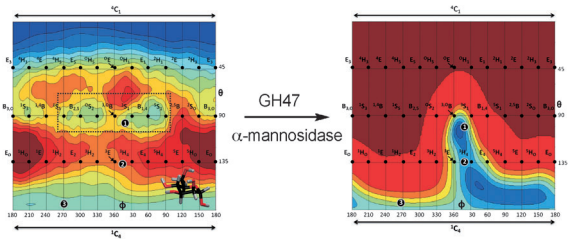

Mannosides in the southern hemisphere: Conformational analysis of enzymatic mannoside hydrolysis informs strategies for enzyme inhibition and inspires solutions to mannoside synthesis. Atomic resolution structures along the reaction coordinate of an inverting α-mannosidase show how the enzyme distorts the substrate and transition state. QM/MM calculations reveal how the free energy landscape of isolated α-D-mannose is molded on enzyme to only allow one conformationally accessible reaction coordinate.

Computational Chemistry

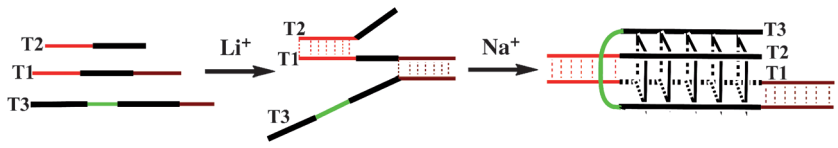

In my (DNA) dreams: A tri-G-quadruplex was constructed from three strands (T1–T3) of DNA using duplex formation to guide the G-rich tracts into close proximity with the addition of Li^+ ions (see scheme). The defined G-quadruplex structure was formed upon addition of Na^+ ions and characterized by gel electrophoresis and spectroscopy.

DNA Structures

The German Chemical Society (GDCh) invites you to:

Angewandte Anniversary Symposium

125 JAHRE Eine Zeitschrift der Gesellschaft Deutscher Chemiker

GDCh

Tuesday, March 12, 2013

Henry Ford Building / FU Berlin

Speakers


Carolyn R. Bertozzi


François Diederich


Alois Fürstner


Roald Hoffmann (Nobel Prize 1981)


Susumu Kitagawa


Jean-Marie Lehn (Nobel Prize 1987)


E.W. "Bert" Meijer


Frank Schirrmacher (Publisher, *FAZ*)


Robert Schlögl


George M. Whitesides


Ahmed Zewail (Nobel Prize 1999)

More information:

Freie Universität Berlin

angewandte.org/symposium

WILEY-VCH

GDCh Gesellschaft Deutscher Chemiker

PSJ_12_42497_5_gu

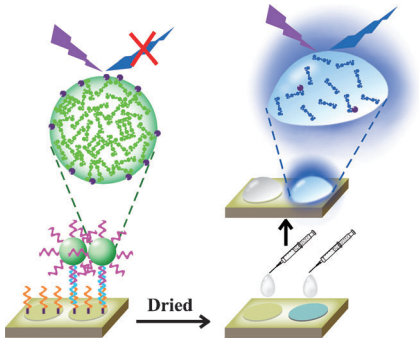

High and dry fluorescence: Fluorogenic nanospheres (green, see scheme) are conjugated to DNA (pink) and used to detect target DNA (aqua). Upon addition of *N*-butylmorpholine (droplet), the nanospheres dissolve, releasing fluorophores, and intense blue fluorescence is emitted at the site of DNA hybridization. The separation of DNA hybridization and signal amplification gives high sensitivity (100 zmol) and selectivity.

Fluorescent Probes

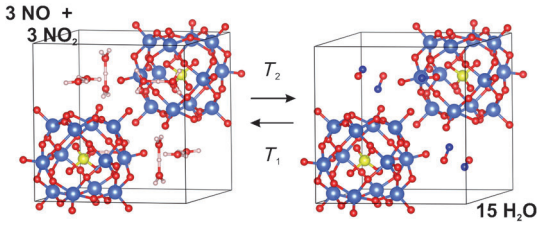

Free-energy calculations indicated that the NO_x adsorption process on heteropolyacids is entropy-driven, as more gas molecules are released than adsorbed by substitution of $H_5O_2^+$ with NO^+ species. P yellow, W light blue, O red, H pink, N small dark blue spheres.

Nitrogen-Oxide Adsorption

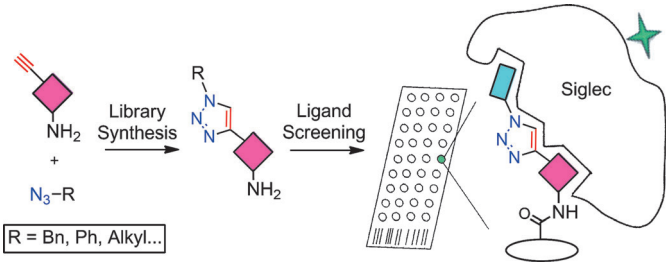

Click 'n' chips: Azide and alkyne-bearing sialic acids (purple diamond; see picture) were subjected to high-throughput click chemistry to generate a library of sialic acid analogues. Microarray printing of the library and screening with the siglec family of sialic-acid-binding proteins, led to the identification of high-affinity ligands for siglec-9 and siglec-10.

Cell Targeting

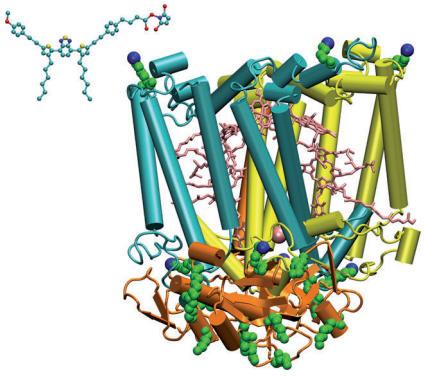

Light machine: The simplest photosynthetic protein able to convert sunlight into other energy forms is covalently functionalized with a tailored organic dye to obtain a fully functional hybrid complex that outperforms the natural system in light harvesting and conversion ability.

Hybrid photosynthetic complexes

Supramolecular Chemistry

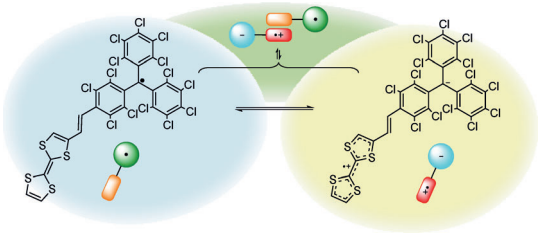

An organic switch: An open-shell dyad, consisting of an electron acceptor perchlorotriphenylmethyl radical unit linked to an electron π-donor tetrathiafulvalene unit through a vinylene π-bridge, was synthesized (see picture). The self-assembly of the dyad in solution induced by its intramolecular electron transfer was studied.

Bulk Water Modeling

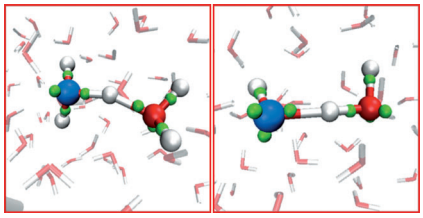

Easy come, easy go: LEWIS, a new model of reactive and polarizable water that enables the simulation of a statistically reliable number of proton hopping events in aqueous acid and base at concentrations of practical interest, is used to evaluate proton transfer intermediates in aqueous acid and base (picture, left and right, respectively).

Supramolecular Catalysis

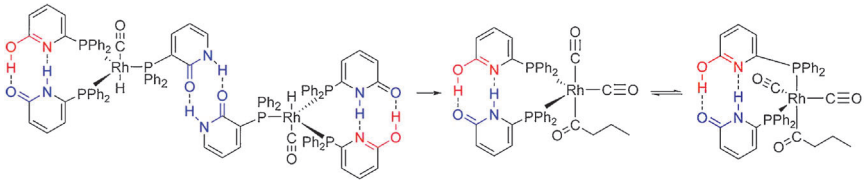

The structural integrity and flexibility provided by intermolecular hydrogen bonds leads to the outstanding properties of the 6-diphenylphosphinopyridin-(2*H*)-1-one ligand (see scheme) in the rhodium-catalyzed hydroformylation of terminal alkenes, as demonstrated by the combination of spectroscopic methods and DFT computations. Hydrogen bonds were also detected in a competent intermediate of the catalytic cycle.

Therapeutic Nanoparticles

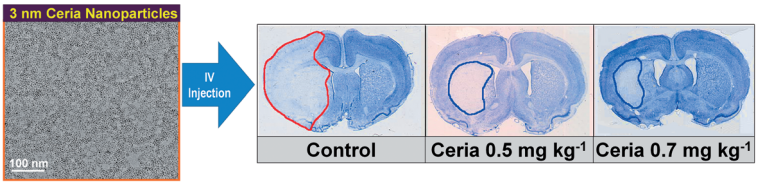

Uniform 3 nm-sized ceria nanoparticles can protect against ischemic stroke by scavenging reactive oxygen species (ROS) and reducing apoptosis. PEGylated ceria nanoparticles showed protective effects against ROS-induced cell death in vitro. Optimal doses of ceria nanoparticles reduced infarct volumes and the rate of ischemic cell death in vivo.

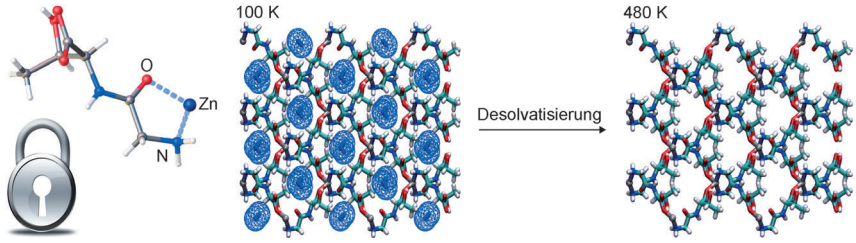

Metal–Organic Frameworks

Pepped up: Notwithstanding the intrinsic conformational flexibility of peptides, [Zn(Gly–Thr)$_2$] behaves as a robust porous metal–organic framework thanks to the rigidity introduced by the use of Gly–Thr (see scheme). This rigidity arises from the sequence of amino acids in the dipeptide that locks its conformational flexibility in the framework.

Spin Crossover

Round and round: A mononuclear Fe^{II} complex (see picture) with an N_4S_2 coordination set has been characterized in four polymorphic forms. Two of the polymorphs display four-site cooperative spin crossover (SCO), shown conclusively by the crystal structure of a fully ordered 1:3 high-spin/low-spin state. The presence of S donor atoms in SCO-active compounds is unusual, and further investigation of Fe^{II} complexes for SCO activity is warranted.

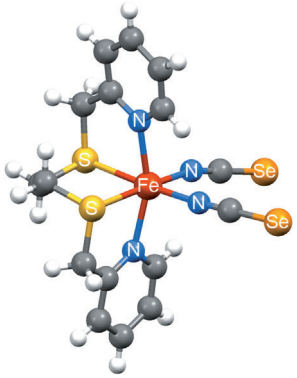

Sensors

There's something in the air ... A nanocomposite consisting of well-dispersed SnO_2 and Pt nanoparticles on reduced graphene oxide (see the high-resolution TEM image) exhibited very high responses to hydrogen at concentrations between 0.5 and 3% in air, with response times of 3–7 s and recovery times of 2–6 s. The sensor was prepared by a straightforward microwave-assisted non-aqueous sol–gel approach.

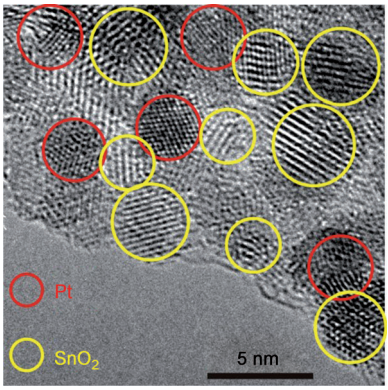

Molecular Chirality

Beef up the signal: Induced resonance Raman optical activity (IRROA) in the presence of a europium complex enabled the detection of molecular chirality (see picture) with a 10^4-fold increase in sensitivity relative to that observed with conventional nonresonant vibrational ROA. The method can thus be used as a sensitive tool for the determination of the absolute configuration and enantiomeric excess of organic and biologically relevant compounds.

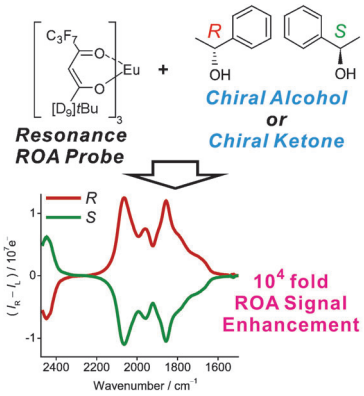

Gel–Air Electrodes

A salt and battery: The combination of single-walled carbon nanotubes (SWNTs) and an ionic liquid (IL) cross-linked network gel (CNG) allows the conventional three-phase reactive interface to be expanded to the whole cross-linked network (see picture). Thus, it integrates high specific energy and specific power with the feasibility of operating in ambient air.

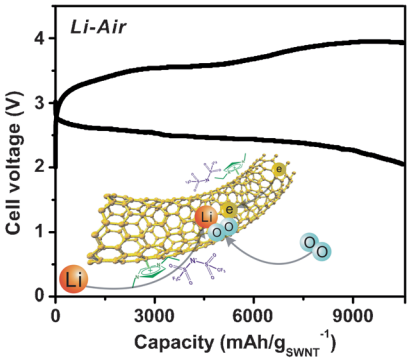

π-Conjugated Polymers

To tilt or not to tilt: The crystal structure for bulk P3HT (phase I) was determined by "multi-technique crystallography", which combines X-ray diffraction, solid-state NMR spectroscopy, and DFT calculations. The results showed that this semiconducting polymer crystallizes in the monoclinic space group $P2_1/c$ with nontilted π-stacks at a distance of 3.9 Å (see picture).

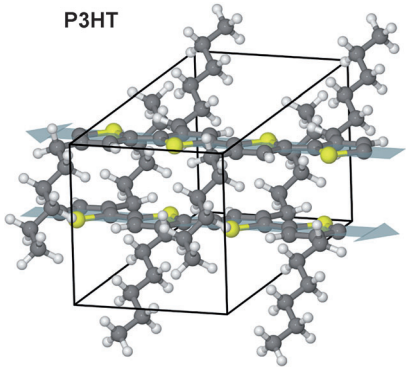

Bioorganic Chemistry

It all clicks into place: A potent telomere-targeting small molecule has been identified by using the copper-free 1,3-dipolar cycloaddition of a series of alkyne and azide building blocks catalyzed by a non-Watson–Crick DNA secondary structure (see picture). This method rapidly identifies, otherwise unanticipated, potent small-molecule probes to selectively target a given RNA or DNA.

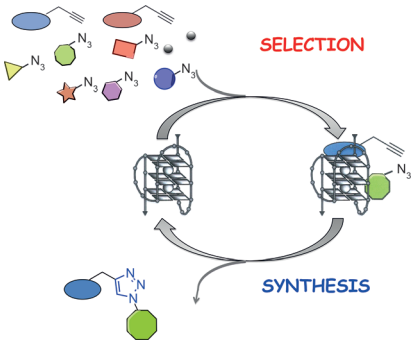

Photoelectrochemistry

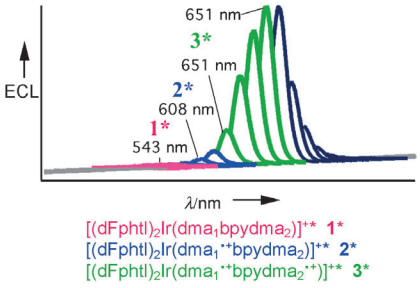

Improved luminophore: The electrochemiluminescence (ECL) of an iridium complex self-enhanced up to 16 times is reported. Three excited states were observed in the emission spectra (see picture). The ECL efficiency of this complex is the highest reported for an iridium complex.

An aureate dye: Confined electromagnetic fields in DNA-templated gold nanoparticle dimers were tuned to engineer the fluorescence properties of organic dyes in water (see picture). Purified suspensions of hybrid metal–organic chromophores featured unprecedented photophysical properties, such as a short lifetime and low quantum yield but high brightness.

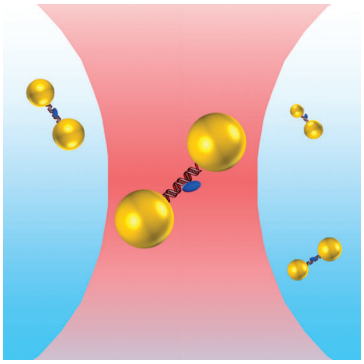

Photochemistry

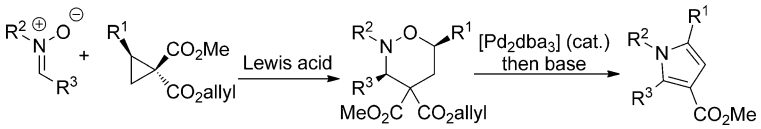

Ring the changes: The cycloaddition of nitrones with 1-carboallyloxy-1-carbomethoxycyclopropanes yields tetrahydro-1,2-oxazines, which in turn undergo a Tsuji dehydrocarbonylation to give dihydro-1,2-oxazines (see scheme; dba = dibenzylideneacetone). Addition of base to this reaction mixture results in clean conversion to pyrroles. The result is a flexible three-component strategy for the synthesis of tetrasubstituted pyrroles.

Pyrrole Synthesis

Excellent tolerance: Stable acylboronates equipped with *N*-methyliminodiacetyl (MIDA) boryl groups (**[B]**) were prepared by using a sequence of oxidative manipulations at the boron-bound carbon center (green in scheme). Chemoselective transformations of these acylated organoboron building blocks yielded a range of multifunctionalized boron derivatives and supplied access to valuable borylated heterocycles (see scheme).

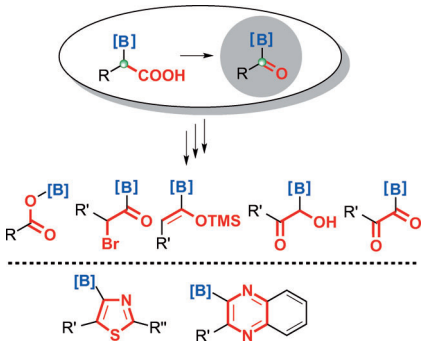

Synthetic Methods

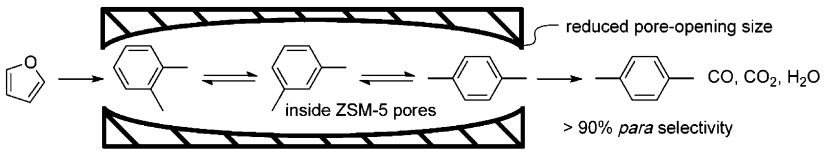

Pores for thought: Chemical liquid deposition of silica onto ZSM-5 catalysts led to smaller pore openings that resulted in >90% selectivity for *p*-xylene over the other xylenes in the catalytic fast pyrolysis of furan and 2-methylfuran (see scheme). The *p*-xylene selectivity increased from 51% with gallium spray-dried ZSM-5 to 72% with a pore-mouth-modified catalyst in the pyrolysis of pine wood.

Heterogeneous Catalysis

Synthetic Methods

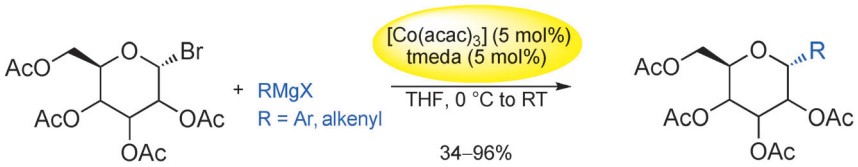

Cobalt, the catalyst of choice: The diastereoselective cobalt-catalyzed cross-coupling of 1-bromo glycosides and aryl or vinyl Grignard reagents is described. A convenient and inexpensive catalyst, $[Co(acac)_3]$/tmeda (acac = acetylacetonate, tmeda = *N*,*N*′-tetramethylethylenediamine), gives full α selectivity in the mannose and galactose series, and an α selectivity in the glucose series with α/β ratios of 1.3:1–3:1.

Glycosides

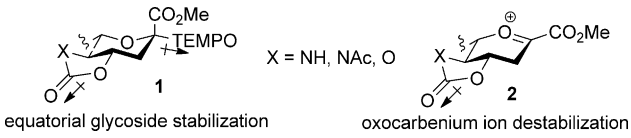

At a moment's notice: Thermal equilibration of **1** and mass spectral analysis of sialyl phosphates suggest that the 4*O*,5*N*-oxazolidinone and the 4,5-*O*-carbonate systems influence the anomeric effect and the mechanisms of sialidation by virtue of their dipole moment in the mean plane of the pyranose ring. The electron-withdrawing effect destabilizes **2** and promotes associative glycosylation mechanisms. TEMPO = 2,2,6,6-tetramethylpiperidine *N*-oxide.

Expanded Phthalocyanines

Supersized: Three pentaazapentaphyrin derivatives, that is, the superazaporphyrins (SAzPs), as well as a superphthalocyanine (SPc) and a mixed low-symmetry derivative have been prepared and characterized. Decaaryl SAzPs have a distorted $(4n+2)$ π structure and show the Q bands at about $\lambda = 840$–880 nm. These compounds are relatively air stable.

Hydridosilicate σ-Complexes

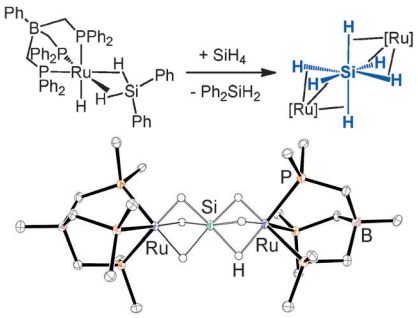

Hydridosilicate anions ($[ArSiH_4]^-$ and $[SiH_6]^{2-}$) were stabilized as ligands in diruthenium Si–H σ-complexes $[\{(PhBP^{Ph}_3)Ru\}_2(\mu\text{-}Cl)(\mu\text{-}\eta^3,\eta^3\text{-}H_4SiAr)]$ (Ar = 2-$MeOC_6H_4$, Mes, Ph) and $[\{(PhBP^{Ph}_3)Ru\}_2(\mu\text{-}\eta^4,\eta^4\text{-}H_6Si)]$ (see picture). These complexes were formed under mild conditions and characterized by single-crystal X-ray diffraction (see picture), NMR and IR spectroscopy, and computational techniques.

Biological macromolecules can be encapsulated into preformed polymersomes by controlled temporary destabilization of the vesicle membrane. The morphology and the size of the polymersome are unchanged after electroporation, suggesting that the polymersome membrane is reformed. The surface charge of the biomacromolecules plays a key role for the electroporation process.

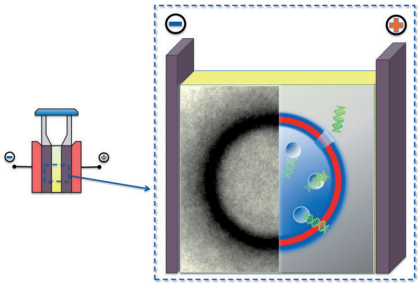

Polymersomes

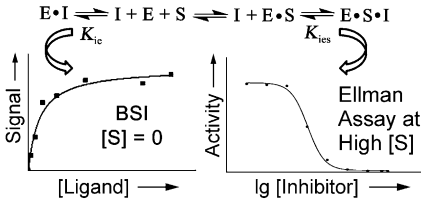

A series of inhibitors of acetylcholinesterase (AChE) have been screened by back-scattering interferometry (BSI). Enzyme levels as low as 100 pM (22 000 molecules of AChE) can be detected. This method can be used to screen for mixed AChE inhibitors, agents that have shown high efficacy against Alzheimer's disease, by detecting dual-binding interactions. E = enzyme, I = inhibitor, S = substrate.

Biosensors

Sowing the seeds: A simple strategy based on self-seeding allows large single crystals of long regioregular poly(3-hexylthiophene) chains to be grown from solution. When appropriately crystallized, materials differing in their degrees of regioregularity and molecular weights formed monoclinic form II crystals with interdigitated hexyl side groups (see picture).

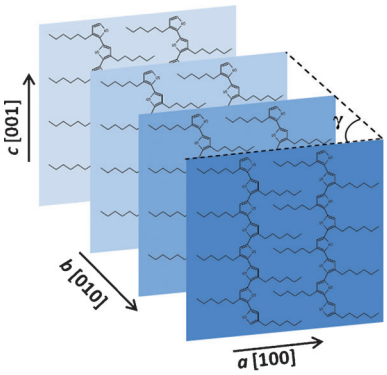

Conjugated Polymers

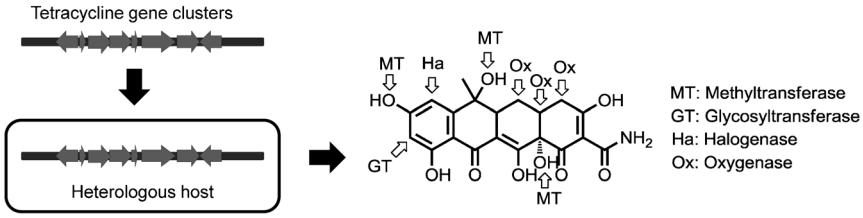

A very accommodating host: Three tetracycline biosynthetic pathways were overexpressed and manipulated in the heterologous host *Streptomyces lividans* K4-114. Through the inactivation of various genes and characterization of the resulting biosynthetic intermediates, new tetracycline-modifying enzymes were identified (see scheme).

Engineered Biosynthesis

Rare-Earth Catalysis

[(NHC)Yb{N(SiMe$_3$)$_2$}$_2$]-Catalyzed Cross-Dehydrogenative Coupling of Silanes with Amines

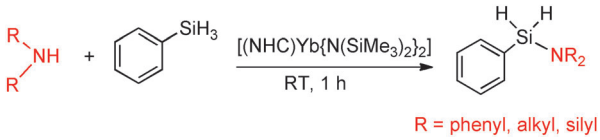

Top cat: [(NHC)Yb{N(SiMe$_3$)$_2$}$_2$] adducts (NHC = N-heterocyclic carbene) are efficient catalysts for catalytic cross-dehydrogenative coupling of silanes with a range of primary and secondary amines to yield silylamines in high yields (82–100%) under mild reaction conditions. The catalytic activity and selectivity of the rare-earth-metal silylamides are modulated by altering the steric bulk of the NHC.

Assay Development

Using Smell To Triage Samples in Point-of-Care Assays

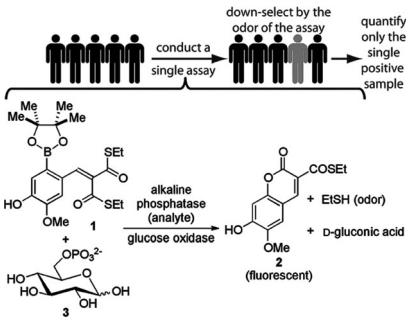

Smell of success: Reagent **1** provides the dual readouts of odor (ethanethiol) and fluorescence (derivative of 7-hydroxycoumarin) and can be used in down-selection assays based on smell and quantitative fluorescence assays of the samples that give a positive result. An important feature of **1** is the matched sensitivity of the two outputs. This reagent is designed for use in resource-limited settings and is demonstrated in assays that detect enzymes.

Gold Catalysis

Anion-Induced Enantioselective Cyclization of Diynamides to Pyrrolidines Catalyzed by Cationic Gold Complexes

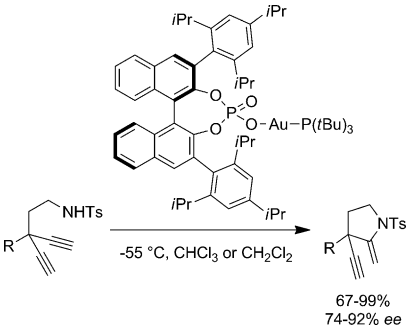

Only chiral anions do the job! Optically active gold complexes derived from substituted binol hydrogen phosphate catalyze the desymmetrizing cyclization of 1,4-diynamides. This reaction provides access to synthetically useful, chiral methylene pyrrolidines with an all-carbon-substituted quaternary stereocenter.

Synthetic Methods

Domino Reactions of Donor–Acceptor-Substituted Cyclopropanes for the Synthesis of 3,3′-Linked Oligopyrroles and Pyrrolo[3,2-*e*]indoles

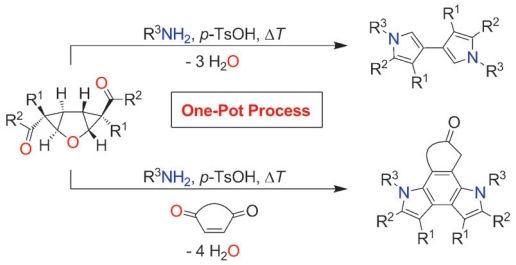

Multiple displacement of oxygen: Electron-rich oligopyrroles and pyrrolo[3,2-*e*]indoles are generated by a domino process induced by donor–acceptor-substituted cyclopropanes. Up to seven molecules of water are eliminated, thus allowing the introduction of nitrogen and aromaticity.

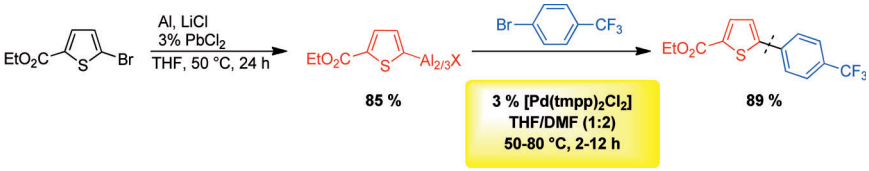

A handsome couple: Through the use of the simple Pd catalyst $[Pd(tmpp)_2Cl_2]$ (tmpp = tris(2,4,6-trimethoxyphenyl)-phosphine) and THF/DMF as solvent, various aryl-, heteroaryl-, benzyl- and alkylaluminum reagents can be readily cross-coupled with aryl or heteroaryl iodides, bromides, and nonaflates, and in special cases even with chlorides and triflates. This cross-coupling tolerates free NH_2 groups, aldehydes, ketones, esters, and nitro functions.

Organoaluminum Reagents

Useful diversity: Quantification of modified tRNA nucleobases in different murine and porcine tissues reveals a tissue-specific overall modification content. The modification content correlates with rates of protein synthesis in vitro, suggesting a direct link between tRNA modification levels and tissue-specific translational efficiency.

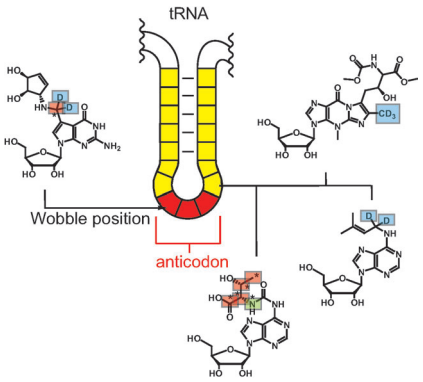

Modified RNA nucleosides

Checking for mistakes: By conjugating a catalytic domain with a guide RNA, deamination activity can be harnessed to repair a specific codon on mRNA. This method can be used for the highly selective repair of point mutations in mRNA by site-selective editing.

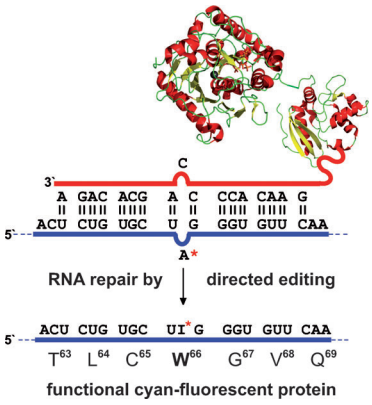

RNA Repair

Supporting information is available on www.angewandte.org (see article for access details).

A video clip is available as Supporting Information on www.angewandte.org (see article for access details).

This article is available online free of charge (Open Access).

This article is accompanied by a cover picture (front or back cover, and inside or outside).

Angewandte Corrigendum

A Multicolor Nanoprobe for Detection and Imaging of Tumor-Related mRNAs in Living Cells

N. Li, C. Chang, W. Pan, B. Tang* **7426–7430**

Angew. Chem. Int. Ed. **2012**, *51*

DOI: 10.1002/anie.201203767

The authors of this communication wish to cite an additional paper as reference [10f]. The complete reference is given here.

[10] a) S. Tyagi, D. P. Bratu, F. R. Cramer, *Nat. Biotechnol.* **1998**, *16*, 49–53; b) S. J. He, B. Song, D. Li, C. F. Zhu, W. P. Qi, Y. Q. Wen, L. H. Wang, S. P. Song, H. P. Fang, C. H. Fan, *Adv. Funct. Mater.* **2010**, *20*, 453–459; c) G. M. Qiao, Y. Gao, N. Li, Z. Z. Yu, L. H. Zhuo, B. Tang, *Chem. Eur. J.* **2011**, *17*, 11210–11215; d) S. P. Song, Z. Q. Liang, J. Zhang, L. H. Wang, G. X. Li, C. H. Fan, *Angew. Chem.* **2009**, *121*, 8826–8830; *Angew. Chem. Int. Ed.* **2009**, *48*, 8670–8674; e) Y. Huang, S. L. Zhao, H. Liang, Z. F. Chen, Y. M. Liu, *Chem. Eur. J.* **2011**, *17*, 7313–7319; f) A. E. Prigodich, P. S. Randeria, W. E. Briley, N. J. Kim, W. L. Daniel, D. A. Giljohann, C. A. Mirkin, *Anal. Chem.* **2012**, *84*, 2062–2066.

